Power-to-Process-Heat in Industrial Combined Heat and Power Plants – Integration of a Large-Scale Thermochemical Energy Storage

Gesa Backofen[1,*] Manuel Würth[1], Annelies Vandersickel[1], Stephan Gleis[1], Hartmut Spliethoff[1,2]

[1] *Chair of Energy Systems, Technical University of Munich, Garching, Germany*
[2] *Bavarian Center of Applied Energy Researach (ZAE Bayern), Garching, Germany*
[*]*Corresponding author. Email: gesa.backofen@tum.de*

***Abstract*—With an increasing share of electricity from renewable energy sources in the German energy market, storage systems are needed to close the gap between production and demand. The thermochemical storage system based on the reversible reaction of CaO and Ca(OH)2 is one of the most promising approaches for high temperature thermal energy storage concepts. In this paper, a concept is developed to integrate a large-scale thermochemical storage system into an industrial heat and power plant. A mixed integer linear problem was created in TOP-Energy to conduct economical optimizations of the industrial heat and power plant with and without storage system. The linearization of the storage system was achieved by a correlation of input and output streams of a stationary CSTR MATLAB model. Hourly simulations for the years 2019, 2030 and 2040 with the help of energy price prognoses proved the economic benefit of the operation with storage system.**

Keywords*—*thermochemical energy storage, industrial heat and power plant, CaO/Ca(OH)2, fluidized bed reactor, mixed integer linear programming.

1. INTRODUCTION

The energy market in Germany is shifting towards a higher share of renewable energies. While more than 50 % of the electricity production in 2020 was already from renewable sources, only 25 % of heat demand was supplied by renewables [1, 2]. With this change in electricity production, and the corresponding marginal cost, there is an increase in periods where buying electricity from the market is significantly cheaper than generating it in a conventional power plant. Industrial combined heat and power (CHP) plants are now facing the problem of having to supply heat according to the demand without being able to operate the power generation optimally to the fluctuating electricity price. This can lead to situations where a CHP plant is unable to shut down its electricity generation and therefore renewable generation has to be regulated for grid stability. Increasing the flexibility of CHPs by integrating energy storage systems can solve this problem and contributes to the goal of decarbonized energy production in Germany [3].

Various cogeneration plants, especially in district heating, are already using sensible water storages to supply the heat demand while electricity generation is not profitable (e.g. [4–6]). Since process heat in industrial CHP plants is needed at pressures up to 150 bar and temperatures between 150 °C and 600 °C [7], low temperature thermal energy storages cannot be used in this case. Options for high temperature energy storages that also have the potential of storing energy in a large scale are molten salt storages, sensible heat storages in solids, phase change material storages (PCMS) and thermochemical energy storages (TCES). Molten salt energy storages are already a state-of-the-art technology and can be found in combination with solar thermal power plants (e.g. [8–11]). A disadvantage of these well-researched storages is the strongly increasing scale up cost due to the expensive heat transfer fluid [8]. PCMSs have been a large research topic over the last 20 years, focusing on material characteristics and laboratory scale storages (e.g. [12–14]). Large problems, however, are posed by low thermal conductivity and flammability in organic PCMSs as well as instabilities like phase separation, subcooling and corrosion in inorganic PCMSs [15][14]. Solid sensible heat storages that can be charged directly from solar power plants or wind farms have been heavily

Copyright © 2022 The Authors. Published by Atlantis Press International B.V.
This is an open access article distributed under the CC BY-NC 4.0 license -http://creativecommons.org/licenses/by-nc/4.0/.

researched (e.g. [16–18]). Companies such as Siemens Gamesa have built multi MWh-scale demonstration storages [19]. However, issues with poor temperature distribution, energy loss during storage intervals and low energy density lead to low volume utilization and therefore strongly increasing investment cost with increasing storage capacity [15].

This paper uses a TCES using the materials calcium oxide (CaO) and calcium hydroxide ($Ca(OH)_2$), as it was presented by Angerer et al. in 2018 and Würth et al. in 2019 [20, 21]. The material is cheap with 15 ct/kWh, non-toxic, well researched, and it has a high reactivity and high energy density [22].

Possible gas-solid reactors for the investigated reaction are fluidized bed reactors (FLBR), fixed bed reactors [23], moving bed reactors [24] and entrained flow reactors. The FBR has the advantages of being able to operate continuously compared to the fixed bed reactor. Furthermore, it has a good heat and mass transfer compared to the moving bed reactor and it needs a relatively low gas velocity compared to the entrained flow reactor [25]. Due to this, the chair of energy systems of the TUM determined the FBR as the most promising reactor for this gas-solid reaction [20, 21].

This article presents the integration of a TCES into an industrial CHP plant. The storage is employed as a power-to-heat application by charging with electricity and discharging steam. The TCES is modelled in MATLAB [26] as an ideal continuously stirred tank reactor (CSTR) model, as presented in [21]. The model is used to find linear relations between the input and output streams of the storage for the integration into an optimization model of the plant using mixed integer linear programming (MILP). The optimization model is implemented in TOP-Energy with the embedded MILP solver Gurobi [28, 29]. With the TOP-Energy model, the economic benefits of the storage system in the year 2019 were simulated. Additionally, the near future was analyzed using a price prognosis from ENTSOG [27].

2. INTEGRATION OF THE STORAGE SYSTEM INTO THE POWER PLANT

2.1. Thermochemical Storage System

The storage system is based on the exothermic hydration of CaO and the corresponding reverse reaction (1). This reaction was first mentioned in the context of energy storages in the 1970s first by Wentworth and later by Ervin [30, 31]:

$$CaO(s)+H_2O(g)\leftrightarrow Ca(OH)_2(s)\ \Delta H_R=-104\ kJ/kmol \quad (1)$$

The storage system consists of two bulk storage silos and two FLBRs as first mentioned by Angerer et al. [21]. For charging the storage, Ca(OH)2 from the first silo is lead to the charging reactor where energy is added to the bulk material by electrical heating elements. This initiates the endothermic dehydration that splits $Ca(OH)_2$ into CaO and steam. Because of their different aggregation states, the products can easily be separated. The steam can be used right away in the according energy system while the CaO is stored in the second silo. The energy is stored in the chemical bond energy of the CaO, which leads to minimal losses. Only sensible heat losses occur due to the hot storage of the material around 500 °C.

When energy is needed, CaO is conveyed into the discharging reactor, where it is combined with steam to conduct the exothermic hydration. The released heat from the exothermic reaction is transferred to built-in heat exchanger tubes that are used as a steam generator. The steam can be utilized as process steam in the energy system and the $Ca(OH)_2$ is stored in the according silo.

2.2. Industrial Heat and Power Plant

The investigated industrial CHP plant generates electricity as well as process steam on a high-pressure and a low-pressure level that can be used to drive steam turbines and engines. A simplified scheme is shown in Fig. 1. Various gas- and coal boilers produce steam at an even higher steam level and directly relax it in a steam turbine to the high-pressure level while generating electricity. Other gas boilers and the gas turbine with heat recovery steam generator directly insert steam into the high-pressure level. Between the high-pressure and the low-pressure level, there are different steam turbines and steam engines along with a relaxation valve. Low-pressure steam that is not directed to the industrial park can be used to power a condensing turbine.

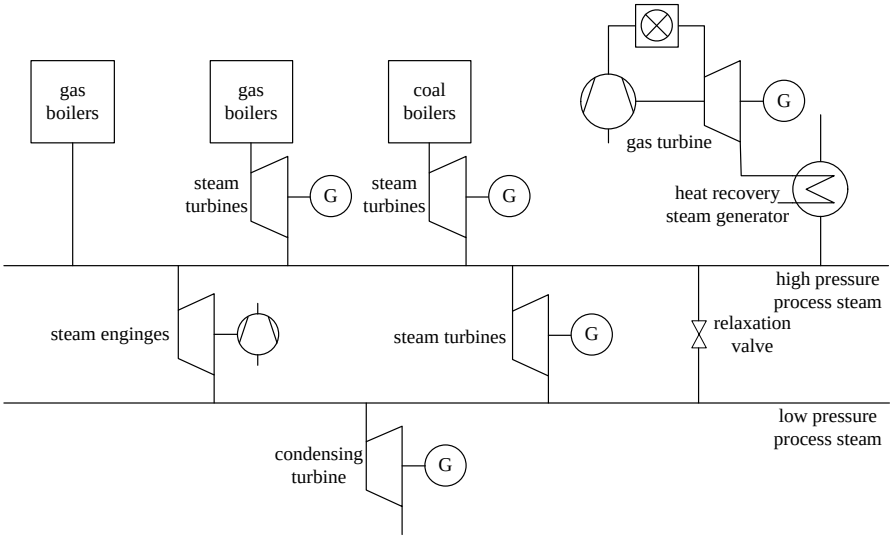

Figure 1. Schematic diagram of the industrial heat and power plant

2.3. Integration of Charging System

In this paper, a storage system with two 100 m³ reactors with 50 m³ fluidization zones each is considered. Relevant input data for the storage simulation is listed in TABLE 1. For integrating the storage system, all storage input and output streams must be connected with the industrial energy system, as is schematically shown in Fig. 2.

The most important energy stream that goes into the charging reactor is the power for the electrical heating. At full load, a maximum electrical power of 18.8 MW goes into the heating pipes. The electricity can be either obtained directly from the electrical grid or from the power that is generated in the turbines. The solid reaction material is conveyed from the Ca(OH)2 bulk storage into the reactor. At the same time, fluidization steam that is needed to fluidize the material is sent to the reactor. The fluidization steam is taken from the low-pressure process steam level, which then determines the pressure inside the FLBR. The endothermic reaction leads to splitting up Ca(OH)2 into CaO and steam.

The enthalpy is stored in the chemical bond energy chemical reaction enthalpy is stored in the chemical bond energy of the CaO. When considering the temperature changes, this leads to a total enthalpy difference between the solid materials in full load of 9.6 MJ/s. After the reaction, the CaO is directed towards the second bulk storage silo for later use. The other 9.2 MW of the input heating energy is converted into the reaction steam during the chemical reaction. This clarifies the importance of the reaction steam being used

Table 1. Simulation Parameters chemical reaction

Simulation parameters	Hydration	Dehydration
Reactor volume [m³]	100	100
Bed volume [m³]	50	50
Height of the bed [m]	1.5	1.5
Heat transfer surface area [m²]	1347.6	1347.6
Heat transfer coefficient [W/m²K]	138-295	138-295
Fluidization velocity at inlet [m/s]	0.3	0.15
Conversion at inlet [-]	0.1	0.9
Mass flow of solids at inlet [kg/s]	15	10.7
Mass flow working fluid [kg/s]	11.1	-
Temperature electric heaters [°C]	-	675

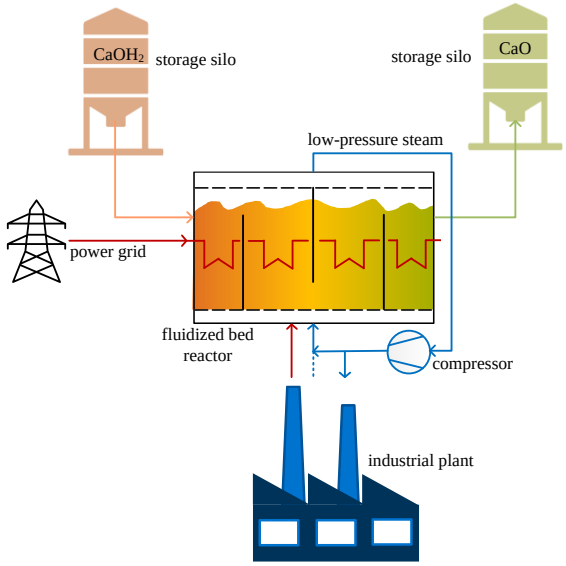

Figure 1. Integration of the charging system

in the industrial energy system. A specific amount of the reaction steam is run through a compressor and circulated back into the reactor to fill up the fluidization steam. Therefore, the majority of the reaction steam is used as low-pressure process steam after being cleared from particles through a cyclone and downstream filter system.

2.4. Integration of the Discharging System

The integration of the discharging system is shown in Fig. 3. For discharging, the high enthalpy storage material is fed into the reactor and fluidized using steam as a fluidization agent. The fluidization steam is drawn from the low-pressure steam level, which has the advantage that it is always available. The elevated pressure of the steam is not wanted in the discharging process. Higher pressures in the reactor lead to a higher equilibrium temperature and therefore elevated reactor and steam temperatures. Hence, the steam is relaxed to slightly above atmospheric conditions before entering the reactor. Combining the CaO and the fluidization steam initiates the exothermic reaction. The heat from the exothermic reaction is transferred to the working fluid in the heat exchanger tubes. The produced 31.5 MJ/s overheated steam is adjusted to the necessary temperature by injection cooling and is then used as high-pressure steam in the industrial plant.

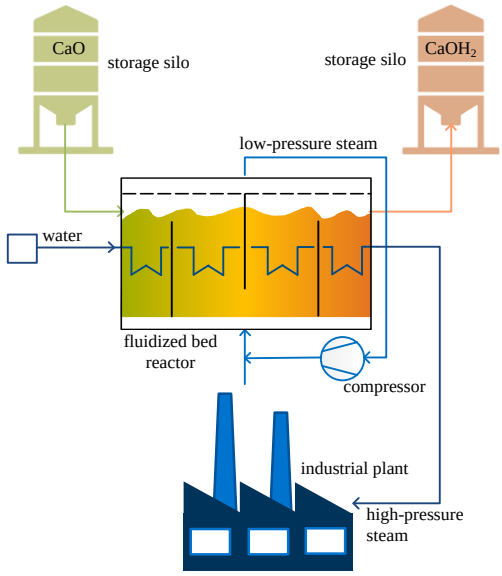

Figure 3. Integration of the discharging system

3. MODELLING OF THE STORAGE SYSTEM

The investigated industrial CHP plant is modelled in TOP-Energy, which is a software for the optimization of energy systems [29]. It uses MILP with the according solver from Gurobi [28]. Each machine is represented by its characteristics such as part and full load performance, dependences between input and output streams, starting costs, and thermodynamic values. Every equation of the optimization system must be linear due to the used mixed integer linear solver. To implement the storage system into the existing simulation, a linear storage model had to be created.

The stationary CSTR MATLAB [26] model that was presented in [21] is used to calculate the linear equations to clarify the relations between input and output parameters for the MILP formulation. The MATLAB model describes the storage reaction in the FLBR with all its input and output streams. As described in [21], the model contains the assumption that all solids in the reactor are perfectly mixed and that there is no temperature distribution between gas and solids within the reactor. The calculation is based on three unknown variables which are the conversion of the chemical reaction, the temperature in the reactor, and the temperature of the work fluid at the end of the heat exchanger tubes. The variables are determined within an equation system including the reaction kinetics, the energy balance around the reactor, and the energy balance around the work fluid. The equation system is solved using the MATLAB lsq-nonlin solver. All other variables can be either calculated directly through the input parameters or post processed from the three solved variables.

As the CSTR MATLAB model is mathematically too complex to form a MILP problem, characteristics for the specific use case are calculated via looping the

model in an executive MATLAB code. The start input parameters like temperature, pressure and geometrics are presented in TABLE 1. To achieve an energy efficient reactor simulation, an additional Ebsilon Professional model is connected to the CSTR MATLAB model. Ebsilon Professional is a software for simulating circuits of power engineering plants by Steag [32]. This Ebsilon model considers the input and output steam streams and calculates the share of steam that can be reused for fluidization purposes. The executive MATLAB code connects both models, where the steam parameters are transferred and iteratively adjusted. In the charging case, the temperature of the electric heaters is varied from 675 °C to the equilibrium temperature in 5 K steps. For each step, the input mass flow of solids that lead to an end conversion of 90 % is identified by an iterative approach. Throughout all steps, the geometry of the reactor and the inside pressure as well as the input fluidization steam flow and the fluidization velocity remain constant. Thereby a damped PI controller using the conversion as the control result regulates the mass flow. The results of the specified calculations are the input solid mass flow, the output solid mass flow, and the fluidization steam output in relation to the input electrical power as depicted in Fig. 4.

The same procedure is used for the discharging case. Here the mass flow of the working fluid is calculated iteratively in connection with a varied input mass flow of solids. The PI controller regulates the working fluid mass flow. The pressure and temperature of the input working fluid that can be used as high-pressure process steam in the industrial plant are held constant during calculations. The results are shown in Fig. 5, where the mass flows of solid output, process steam output, and fluidization steam input are set into relation with the input solid mass flow.

The results of the iterative calculations can then be used as a correlation between input and output values for the linear programming. In the optimization, the

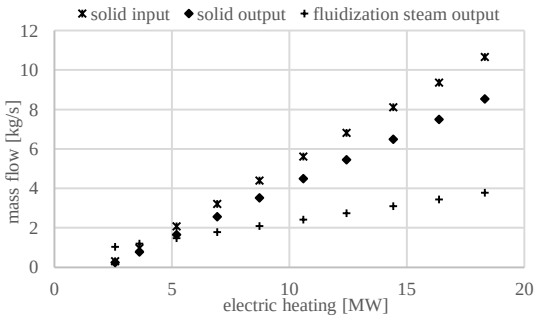

Figure 4. Correlation between input and output data of the charging system

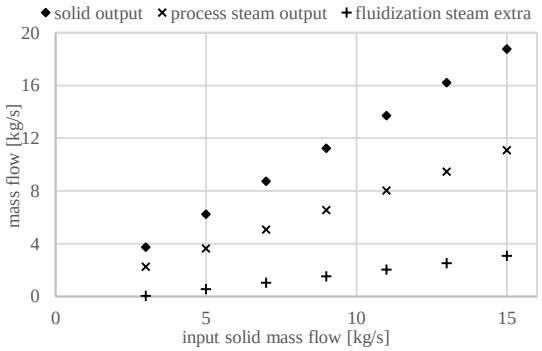

Figure 2. Correlation between input and output data of the discharging system

solver can pick each point of the linear correlations and then determine the corresponding values. Different equation systems were developed for the charging process, the discharging process, and the bulk storages. The charging and discharging processes do not only include the reactors itself but also the electrical power for the compressor and the recycling of the fluidization steam. In the storage components, the storage capacity and the amount of material in the storage at the beginning of the simulation as well as the maximum charging and discharging capacity are set as input values. Integration of the start values combined with the in- and outgoing streams adjusts the storage level during the simulation. Access by external constraints like initial costs and availabilities is enabled for all new equation systems.

4. SIMULATION OF THE STORAGE INTEGRATION

The simulations are executed in TOP-Energy, where the developed storage model is integrated into the industrial CHP plant model. TOP-Energy has the option to implement time series to construct optimization problems throughout specific time spans. Additional time dependent constraints like energy prices, energy demands, and maintenance time slots can therefore be considered. The industrial CHP plant provided hourly steam demand data for the year 2019. Consequently, the year 2019 was chosen to be simulated as well as the years 2030 and 2040 with according prognoses. The optimal operation mode of the plant with and without storage integration is calculated to demonstrate the economic benefits that the storage system could allow. The utilized energy price data is outlined in the next paragraph. To reach an appropriate calculation time while remaining as precise as possible, a rolling horizon algorithm with a 48 h forecast horizon and a 12 h result take over.

4.1. Energy Prices

The electricity prices from the year 2019 are listed hourly in [33] and can be seen in Fig. 6 together with other energy prices that are used in the simulation. With a medium day ahead market price of 36,64 €/MWh in 2019, the electricity for industrial utilization was comparably high to the 28,20 €/MWh in 2016 [34]. After a decreasing electricity price for ten years from 2006 to 2016, the price was rising for two years and is now (in 2020) again at the lowest level since 2002 [34]. The natural gas price is listed monthly in [35] and has a medium value of 15,99 €/MWh HHV in 2019. This price level is very low compared to the years from 2010 to 2015 and in 2019 reached the same level as pre-2010 [36]. The import coal market price is extracted from [37]. Historical data from [38] show, that since a peak in coal price in 2008, the price decreased to the low level of 7.22 €/MWh LHV in 2019. Lastly, the yearly medium of the CO_2 spot market price is listed in [39] since 2010, where it started very low and quadrupled by the year 2019. More detailed data that is used for the simulation is extracted from [40] and is also shown in Fig. 6. For the prognosis, the values from TYNDP 2020 Scenario Report are used and summarized in Table 2 [27]. To have a realistic fluctuation of energy prices, the fluctuations from 2019 are calculated proportionally to the prognosis prices.

Table 2. Prognosis energy prices [27]

Year	Gas price [€/MWh]	Coal price [€/MWh]	CO_2 price [€/tCO_2]	Electricity price [€/MWh]
2019	15.99	7.22	24.70	36.64
2025	23.26	13.64	23	51
2030	24.88	15.48	35	49
2040	26.32	24.88	80	38

4.2. Results

The optimizations proved that integrating the storage system into the industrial CHP plant shows economic benefits in operating costs for all simulated years. Table 3 presents the full load cycles and operating hours that indicate the storage activity. In the year 2019, the storage system would have been active for nearly half the year. The activity is significantly increased in the prognosis year 2030 with more full load cycles and operating hours. The operating hours in 2040 almost doubled the value from 2019 while the full load cycles more than tripled. This means that not only has the activity but also the intensity of the storage use increased. This behavior is explained by the price development within the prognosis. The further the prognosis goes into the future, the more expensive natural gas, coal, and CO_2 become. At the same time, the electricity price increases for the first years after 2019 and then decreases again. The rise in fossil fuel price explains the higher activity of the storage system in both future scenarios. The reason is that steam production through discharging the storage competes with fossil fuel combustion. The additional low electricity price in 2040 leads to the even better values of the storage system as the storage is charged by electricity. This underlines the influence of the relation between fossil fuel prices and electricity prices on storage activity.

The strong influence of the electricity price can also be seen in Fig. 7. This shows the charging and discharging behavior of the storage in connection to

Table 3. Simulation results on the subject of storage activity

	2019	2030	2040
full load cycles [-]	104.1	188.3	382.5
operating hours [h]	4081	7058	8027

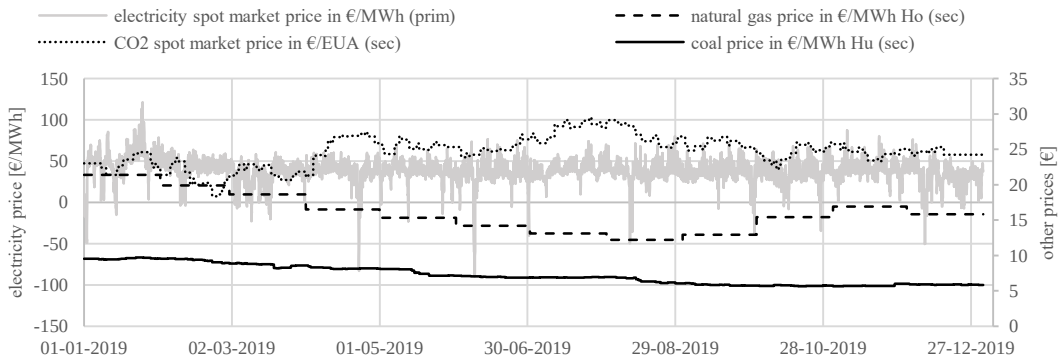

Figure 3. Energy prices in 2019

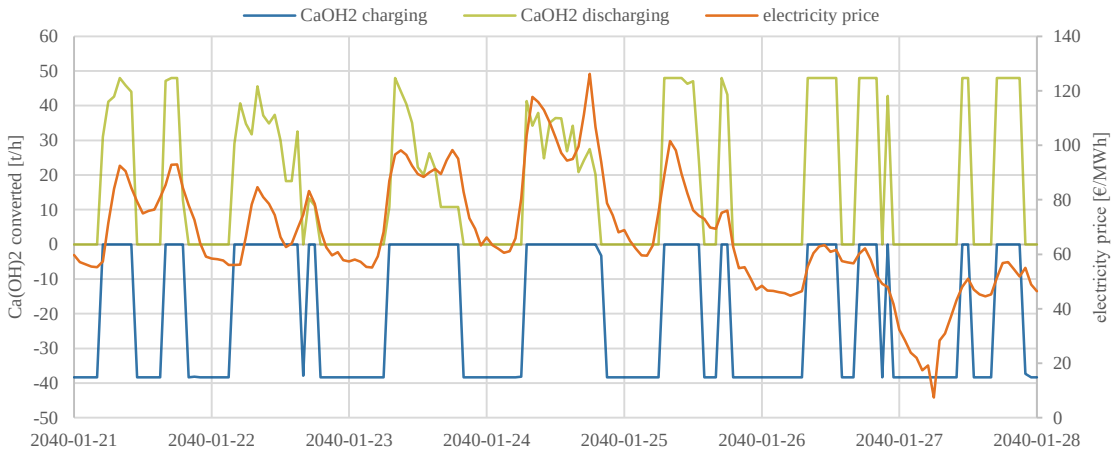

Figure 7. Simulation results of charging and discharging behavior in dependence of the electricity price

the electricity price for an example week in 2040. The charging behavior noticeably follows the electricity price. Electrical charging is conducted corresponding to low energy prices and operates almost consistently in full load. According to that, the storage uses higher electricity prices for discharging. Here a significant number of hours in part load is visible which can be explained with the connection to the steam levels. The steam demand always has to be supplied precisely. Overproduction is only possible if the extra steam amount fits to the characteristics of the condensation turbine. Furthermore, the fossil steam generators follow their technical characteristic such as minimum load and maximum load change. This makes it clear that steam production consists of various variables that make the integration of generated steam complex.

Fig. 8 points out the financial benefit of the storage integration broken down into different cost sources. The graph shows the difference between costs with and without storage. Positive differences represent higher expenses due to the storage operation while negative differences stand for benefits. According to the storage activity, the total benefit increases from 2019 to 2040. The majority of the benefit comes from reducing fossil fuels for combustion by supplying the steam demand from the storage. At the same time, a significant part of these savings is compensated by an increasing electricity cost due to electrical storage charging. Furthermore, reducing steam production from fossil fuels also decreases electricity production from the steam turbines above high-pressure level. This can be seen in the diminished electricity revenue. Lastly, initial costs are higher in the simulation with storage because of the frequent starts of the storage reactors.

With the rough assumption that the total benefit would increase linearly in the years between 2030 and 2040, an investment into the storage system in the year

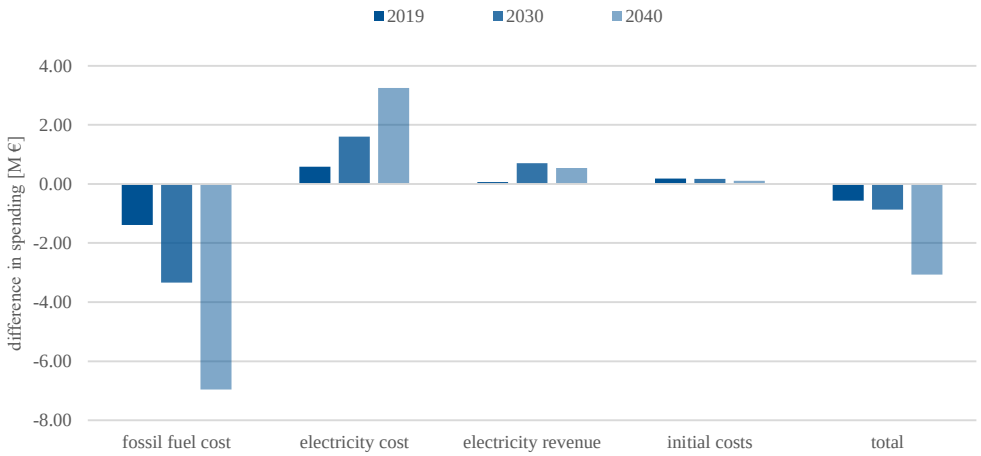

Figure 4. Difference in operation cost of the simulation with and without storage

2030 would be paid off after nine years. Hereby the investment costs for the storage system with two FLBRs and two silos are assumed 17 M € referring to [41].

5. CONCLUSION

This work presents the concept of the integration of a thermochemical storage system into an industrial CHP plant. The storage is charged by electrical heating tubes and discharges producing steam via heat exchanger tubes. The integration was realized by implementing the storage into the steam network of the power plant. Low-pressure level steam is used for fluidization and as product and educt for the reversible reaction. High-pressure steam is produced during discharging.

A mixed integer linear model was created for the specific use case of this storage system. The model is based on the correlation between input and output streams of the storage reactors. The correlations were calculated with the help of a stationary CSTR MATLAB model. The storage model was implemented to a MILP of the industrial CHP plant in TOP-Energy. Optimizations were conducted for the economically optimal operation of the industrial CHP plant with and without storage system in the years 2019, 2030 and 2040.

Optimizations showed a significant storage activity and economic benefit in operating costs for all years. With the prognosis that predicts fossil fuel and CO_2 costs to rise drastically, the benefits are the largest in 2040. Considering the rise of the benefit between 2030 and 2040, an investment into the storage system after 2030 pays off in less than ten years.

ACKNOWLEDGMENTS

This research is part of the project „Thermochemische Energiespeicher im Wirbelschichtverfahren für Industrie-anwendungen und Stromerzeugung“ (TWIST) and is funded by the German Federal Ministry of Economic Affairs and Energy (BMWi) under the funding code 03ET1599A according to a decision of the German Federal Parliament.

The title "ACKNOWLEDGMENTS" should be in all caps and should be placed above the references. The references should be consistent within the article and follow the same style. List all the references with full details.

REFERENCES

[1] B. Burger, Net installed electricity generation capacity in Germany [Online], Available: https://www.energy-charts.de/power_inst.htm (accessed: Sep. 17 2020).

[2] Bundesverband erneuerbare Energien e.V., „Ways into the modern energy industry“, original: “Wege in die moderne Energiewirtschaft,” [Online]. Available: https://www.bee-ev.de/fileadmin/Publikationen/Studien/091015_BEE-Branchenprognose_Waerme2020.pdf, 2009.

[3] A. Buttler, J. Hentschel, S. Kahlert, M. Angerer, and H. Spliethoff, „Status Report Flexibility Requirements in the Power Sector“, original: “Statusbericht Flexibilitätsbedarf im Stromsektor,” Schriftenreihe Energiesystem im Wandel, part I, 2015.

[4] C. Maifredi, L. Puzzi, and G. P. Beretta, “Optimal power production scheduling in a complex cogeneration system with heat storage,” AIAA Meeting Paper, vol. 35, pp. 1004–1012, 2000.

[5] A. Stoppato, A. Benato, N. Destro, and A. Mirandola, “A model for the optimal design and management of a cogeneration system with energy storage,” Energy and Buildings, vol. 124, pp. 241–247, 2016.

[6] H. Wang, W. Yin, E. Abdollahi, R. Lahdelma, and W. Jiao, “Modelling and optimization of CHP based district heating system with renewable energy production and energy storage,” Applied Energy, no. 159, pp. 401–421, 2015.

[7] K. Strauß, Power plant technology: to use fossil, nuclear and regenerative energy sources, original: Kraftwerkstechnik: zur Nutzung fossiler, nuklearer und regenerativer Energiequellen, 6th ed. Heidelberg: Springer, 2009.

[8] U. Herrmann, B. Kelly, and H. Price, “Two-tank molten salt storage for parabolic trough solar power plants,” Energy, vol. 29, 5-6, pp. 883–893, 2004.

[9] J. E. Pacheco and R. Gilbert, “Overview of recent results of the Solar Two test and evaluations program,” Renewable and advanced energy systems for the 21st Century, Maui, HI (US), vol. 1999, 1999.

[10] R. I. Dunn, P. J. Hearps, and M. N. Wright, “Molten-Salt Power Towers: Newly Commercial Concentrating Solar Storage,” Proc. IEEE, vol. 100, no. 2, pp. 504–515, 2012.

[11] A. A. Kordmahaleh, M. Naghashzadegan, K. Javaherdeh, and M. Khoshgoftar, “Design of a 25 MWe Solar Thermal Power Plant in Iran with Using Parabolic Trough Collectors and a Two-Tank

Molten Salt Storage System," International Journal of Photoenergy, vol. 2017, pp. 1–11, 2017.

[12] D. Laing, C. Bahl, T. Bauer, D. Lehmann, and W.-D. Steinmann, "Thermal energy storage for direct steam generation," Solar Energy, vol. 85, no. 4, pp. 627–633, 2011.

[13] D. Li, Y. Hu, D. Li, and J. Wang, "Combined-cycle gas turbine power plant integration with cascaded latent heat thermal storage for fast dynamic responses," Energy Conversion and Management, vol. 183, pp. 1–13, 2019.

[14] J. P. Hadiya, and A. K. N. Shukla, "Thermal energy storage using phase change materials: a way forward," Int. J. Global Energy Issues, vol. 41, pp.108-127, 2018.

[15] P. H. Feng, B. C. Zhao, and R. Z. Wang, "Thermophysical heat storage for cooling, heating, and power generation: A review," Applied Thermal Engineering, vol. 166, p. 114728, 2020.

[16] D. Laing, W.-D. Steinmann, R. Tamme, and C. Richter, "Solid media thermal storage for parabolic trough power plants," Solar Energy, vol. 80, no. 10, pp. 1283–1289, 2006.

[17] N. P. Siegel, C. K. Ho, S. S. Khalsa, G. J. Kolb, "Development and Evaluation of a Prototype Solid Particle Receiver: On-Sun Testing and Model Validation," ASME, Journal of Solar Energy Engineering, Vol. 132, 2010.

[18] H.-W. Yuan, C.-H. Lu, Z.-Z. Xu, Y.-R. Ni, and X.-H. Lan, "Mechanical and thermal properties of cement composite graphite for solar thermal storage materials," Solar Energy, vol. 86, no. 11, pp. 3227–3233, 2012.

[19] Siemens Gamesa, Thermal energy storage with ETES. [Online]. Available: https://www.siemensgamesa.com/products-and-services/ hybrid-and-storage/thermal-energy-storage-with-etes (accessed: Sep. 17 2020).

[20] M. Wuerth, M. Becker, P. Ostermeier, S. Gleis, and H. Spliethoff, "Development of a continious Fluidized Bed Reactor for thermochemical Energy Storage Application," ASME, Journal of Energy Resources Technology, Vol. 141, Issue 7, 2019.

[21] M. Angerer et al., "Design of a MW-scale thermochemical energy storage reactor," Energy Reports, vol. 4, pp. 507–519, 2018.

[22] M. Angerer, M. Djukow, K. Riedl, S. Gleis, and H. Spliethoff, "Simulation of Cogeneration-Combined Cycle Plant Flexibilization by Thermochemical Energy Storage," Journal of Energy Resources Technology, vol. 140, no. 2, p. 40, 2018.

[23] M. Schmidt and M. Linder, "Power generation based on the Ca(OH)2/ CaO thermochemical storage system – Experimental investigation of discharge operation modes in lab scale and corresponding conceptual process design," Applied Energy, vol. 203, pp. 594–607, 2017.

[24] M. Schmidt, M. Gollsch, F. Giger, M. Grün, and M. Linder, "Development of a moving bed pilot plant for thermochemical energy storage with CaO/Ca(OH)2," AIP Conference Proceedings, vol. 1734, 2016.

[25] Z. H. Pan and C. Y. Zhao, "Gas–solid thermochemical heat storage reactors for high-temperature applications," Energy, vol. 130, pp. 155–173, 2017.

[26] The MathWorks Inc., MATLAB - MathWorks. [Online]. Available: https://de.mathworks.com/products/matlab.html (accessed: Sep. 18 2020).

[27] ENTSOG, and ENTSO-E, "TYNDP 2020 Scenario Report – Final Report," 2020.

[28] Gurobi, Gurobi Optimizer - Gurobi. [Online]. Available: https://www.gurobi.com/products/gurobi-optimizer/ (accessed: Sep. 18 2020).

[29] gfai tech GmbH, TOP-Energy® - top-energy.de. [Online]. Available: https://www.top-energy.de/ (accessed: Sep. 18 2020).

[30] W. E. Wentworth, E. Chen, "Simple thermal Decomposition Reactions for Storage of solar thermal Energy," Solar Energy, vol. 1977, no. 18, pp. 205–214, 1977.

[31] G. Ervin, "Solar heat Storage using chemical Reactions," Journal of solid state Chemistry, vol. 1977, no. 22, pp. 51–61, 1977.

[32] STEAG System Technologies, EBSILON Professional. [Online]. Available: https://www.steag-systemtechnologies.com/de/produkte/ebsilon-professional (accessed: Sep. 18 2020).

[33] Bundesnetzagentur, Market date, original: Marktdaten.[Online]. Available: https://smard.de/home/downloadcenter/download_marktdaten (accessed: Sep. 18 2020).

[34] B. Burger, Annual electricity spot market prices in Germany [Online]. Available: https://www.energy-charts.de/price_avg.htm?year=all&price=nominal&period=annual (accessed: Sep. 18 2020).

[35] Bundesministerium für Wirtschaft und Energie, Energy data: Complete edition, original: Energiedaten: Gesamtausgabe. [Online]. Available: https://www.bmwi.de/Redaktion/DE/Artikel/Energie/energiedaten-gesamtausgabe.html (accessed: Sep. 18 2020).

[36] Bundesamt für Wirtschaft und Ausfuhrkontrolle, Natural gas statistics, original: Erdgasstatistik.

[Online]. Available: https://www.bafa.de/DE/ Energie/Rohstoffe/Erdgasstatistik/erdgas_node.html (accessed: Sep. 18 2020).

[37] finanzen.net, Coal price historical rates in Euro, original: Kohlepreis historische Kurse in Euro. [Online]. Available: https://www.finanzen.net/ rohstoffe/kohlepreis/historisch/euro (accessed: Sep. 18 2020).

[38] Statista, Preiseentwicklung Price development of steam coal until 2019, original: Kraftwerkskohle bis 2019. [Online]. Available: https://de.statista.com/statistik/daten/studie/163040/umfrage/entwicklung-des-preises-fuer-kraftwerkskohle-seit-1975/ (accessed: Sep. 18 2020).

[39] European Energy Exchange AG, EEX EUA Primary Auction Spot - Download. [Online]. Available: https://www.eex.com/en/market-data/environmental-markets/eua-primary-auction-spot-download (accessed: Sep. 18 2020).

[40] finanzen.net, CO2 European Emission Allowance Price historical rates in Euro, original: CO2 European Emission Allowancespreis historische Kurse in Euro [Online]. Available: https://www.finanzen.net/ rohstoffe/co2-emissionsrechte/historisch (accessed: Sep. 18 2020).

[41] M. Angerer, „Thermochemical storage systems for applications in energy and process engineering", original: "Thermochemische Speichersysteme für Anwendungen in der Energie- und Verfahrenstechnik," Dissertation, Technical University of Munich, Garching, unpublished.